Performance analysis on an integrated three-area thermal AGC system with various wind velocities considering HCSA-optimized PI-TIDN Controller

Naladi Ram BABU⊙ , Tirumalasetty CHIRANJEEVI⊙ ,
Ramesh DEVARAPALLI⊙ and Fausto Pedro GARCÍA MÁRQUEZ⊙

This article investigates the impact of a high-voltage direct-current (HVDC) link and a wind turbine system (WTS) on the dynamics of a three-area thermal automatic generation control (AGC) system. A novel controller, the cascade of proportional-integral (PI) and tilt-integralderivative (TID) with filter coefficient (N) (PI-TIDN) controller is projected. The WTS units are subjected to various wind velocity scenarios, including fixed and random wind velocities. The controller parameters are concurrently enhanced using the hybrid crow search algorithm (HCSA). The system dynamics corresponding to the PI-TIDN controller are superior to those of PIDN and TIDN controllers. Additionally, studies with different wind velocities demonstrate that responses with fixed wind velocities are better than those with random wind velocities. Moreover, integrating WTS units with the thermal system improves dynamics compared to the thermal system alone. It is also apparent that the parallel AC-HVDC system enhances dynamics. Furthermore, sensitivity analysis exposes that the PI-TIDN controller values at nominal settings are vigorous and do not require retuning.

Key words: hybrid crow search algorithm, wind turbine system, high voltage direct current link, thermal unit, sensitivity analysis

N.R. Babu (e-mail: rambabu.nits@yahoo.com) is with Department of Electrical and Electronics Engineering, Aditya University, Surampalem, Andhra Pradesh, India.

T. Chiranjeevi (e-mail: tirumalasetty.chiranjeevi@recsonbhadra.ac.in) is with Department of Electrical Engineering, Rajkiya Engineering College Sonbhadra, U.P., India.

R. Devarapalli (e-mail: Dr.R.Devarapalli@gmail.com) is with Department of Electrical/Electronics and Instrumentation Engineering, Institute of Chemical Technology, Indianoil Odisha Campus, Bhubaneswar 751013, India.

F.P. García Márquez (corresponding author, e-mail: FaustoPedro.Garcia@uclm.es) is with Ingenium Research Group, University of Castilla-La Mancha, Spain.

1.   Introduction

As modern power systems (PS) expand, they have increasingly become complex networks. Ensuring a power balance between generation and demand is crucial. Any imbalance can lead to frequency and power profile abnormalities within the PS. Persistent imbalances can ultimately destabilize the system. Automatic Generation Control (AGC) addresses this issue by maintaining PS frequency and power near nominal values across different control areas [1, 2].

Early AGC research focused on isolated thermal systems [3] and was extended to two-area, three-area, and multi-area thermal systems [4, 5]. Researchers eventually developed practical thermal system models incorporating governor rate constraint (GRC), generation rate constraint (GDB), and droop characteristics.

The constant reliance on fossil fuels for power generation has led to their depletion and raised significant environmental concerns. These issues have ambitiously merged renewable energy sources (RES) into existing systems. Among these RES, solar and wind energy offer substantial advantages. AGC studies have been on two-area systems with the integration of various RES, such as wind turbine systems (WTS), distributed solar thermal systems (DSTS), solar thermal, and geothermal energy [6–9]. However, there has been limited research on AGC studies involving WTS integration in three-area systems. Therefore, further research is needed to explore WTS integration in systems with more than two areas. The impact of different wind velocities, such as fixed and random, on three-area thermal-WTS units has not been studied.

The increasing population and industrialization are driving up power demand each year. All the provincial grids are interconnected to overcome this. Tie-lines transport power between regions, but their capacity has reached its limit and needs to be expanded [10]. The presence of transients in long transmission lines can further degrade system dynamics. Constructing high voltage direct current transmission (HVDC) tie-lines alongside existing AC tie-lines can help meet the rising power demand [11, 12]. Previous studies [13–17] have investigated the HVDC model within a two-area AGC system. However, these AGC studies have primarily focused on two-area systems [18, 19]. Therefore, there is a need to extend these studies to include systems with more than two areas that utilize RES.

The secondary controller design plays a vigorous role in reducing frequency and megawatt power abnormalities. AGC employs classic control (CC) approaches such as I, PID, and PIDN [20]. Many fractional controllers (FC) have been utilized in the literature, with better outcomes than classical approaches [21]. Intelligent controllers such as fuzzy, neural networks [18] and tilt [22,23] are also available. Cascade connections of IC-FC are presented that exhibit better response over single loop IC, FC controllers [24–26]. A cascade combination of PI-tilt-

DN (PI-TIDN) is proposed and its application in AGC of three-area thermal-WTS units has not been reported.

The finest modification of secondary controllers can enhance the system's recital. Classical tuning is laborious, time-consuming, and offers local bests, while evolutionary algorithms (EA) deliver global bests [27–30]. EAs like whale optimization [31], sine cosine [32], ant-lion [33], biogeography [34], bird swarm [23], coyote [35], particle swarm optimization (PSO) [36], cuckoosearch [37], crow search algorithm (CSA) [38, 39], shuffled frog [40, 41], spotted hyena [25, 26] etc., are available for AGC studies. Recent trends have been involving the hybridization of existing algorithms. A recent hybrid algorithm, the hybrid crow search algorithm (HCSA), is available, but its application has not been found in the three areas of thermal-WTS studies [42].

Studies on the controller's sensitivity analysis (SA) at varied values of PS inertia and loading conditions from nominal values are performed by the authors in [2, 4]. However, the SA of the suggested PI-TIDN controller with HCSA has not been reported. From the overhead, the intentions are:

1. To develop a three-area thermal system amalgamated with WTS and HVDC tie-line.

2. To assess system dynamics with PIDN, TIDN, and the proposed PI-TIDN controller.

3. To apply the HCSA technique to AGC studies.

4. To study the impact of various wind velocities on WTS units.

5. To study the effect of WTS and HVDC units.

6. To perform sensitivity analysis of PI-TIDN controllers.

2. System examined

The examined system encompasses a three-area thermal system integrated with a WTS unit in all the areas and is shown in Fig. 1a. 3%/min GRC, GDC, and 4% droop are considered. As power demand continues to rise among interconnected areas, it becomes necessary to enhance tieline power capacity by adding a high voltage direct current (HVDC).

The energy stored in the HVDC link, considering inertia emulation control strategies, is used for frequency adjustment, and their associate AC power equation ($\Delta P_{\text{tie}\,i-j\,\text{AC}}$) with areas (i, j) is as follows [15]:

$$\Delta P_{\text{tie}\,i-j\,\text{AC}} = \frac{2\Pi T_{ij}}{s}\big(\Delta F_i - \Delta F_j\big), \tag{1}$$
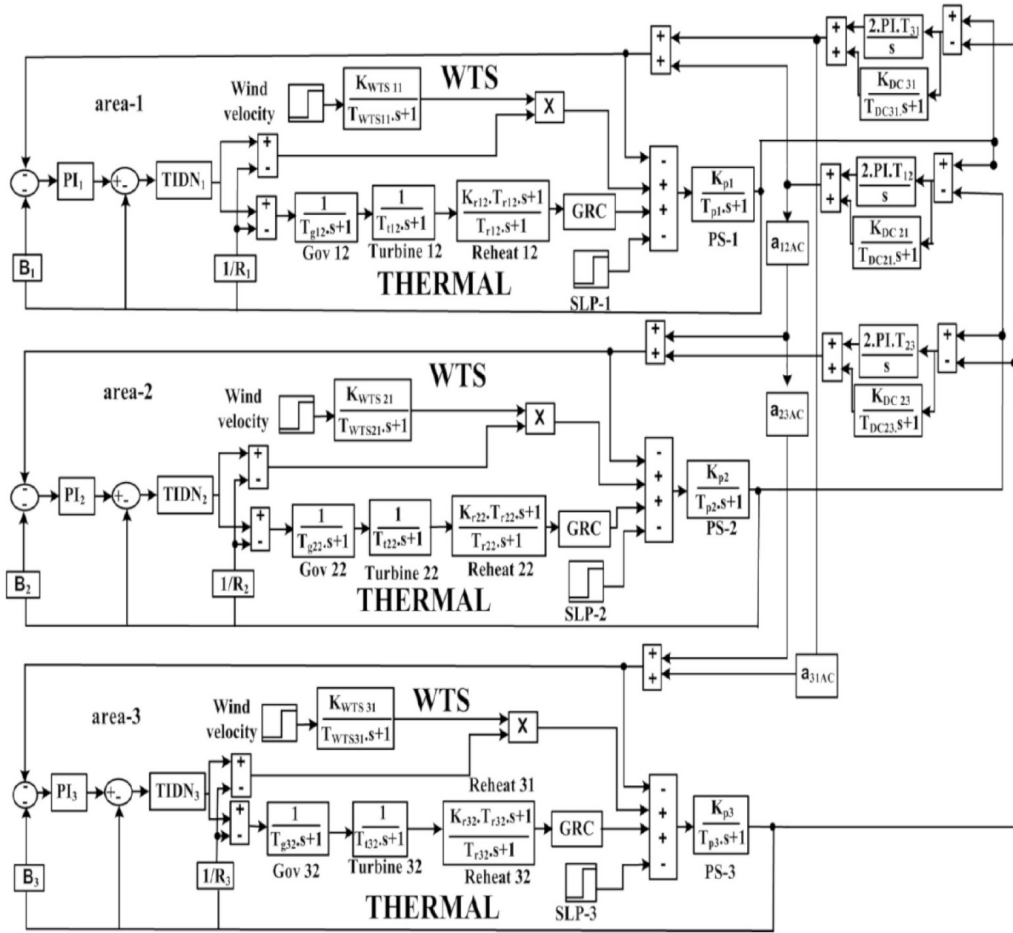
(a)
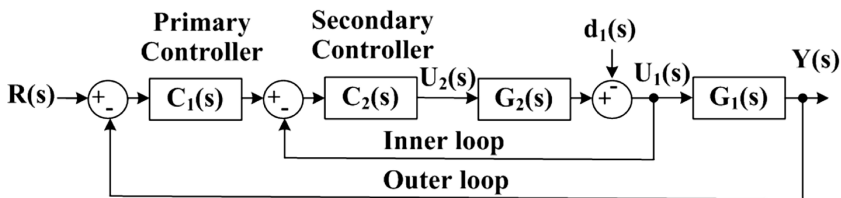
(b)

Figure 1: (a) The investigated three-area thermal-WTS system with HVDC integration;
(b) Bock diagram of cascade control

where time constant (T_{ij}), and ΔF is the frequency change,

$$\Delta P_{\text{tie } i-j \text{ HVDC}}(s) = (2\pi T_{\text{eqv}}/s) \times \left(\Delta F_i(s) - \Delta F_j(s)\right),$$

where

$$T_{\text{eqv}} = \left(\frac{T_{ij,\,\text{DC}} \times T_{ji,\,\text{DC}}}{T_{ij,\,\text{DC}} + T_{ji,\,\text{DC}}}\right) \quad \forall i, k = 1, 2, 3, \tag{2}$$

$T_{ij\text{DC}}$ and $T_{ji\text{DC}}$ time constant of converter and inverter end,

$$\Delta P_{\text{tie } ij \text{ AC}} = \Delta P_{\text{tie } ij \text{ AC}} + \Delta P_{\text{tie},i-j,\,\text{HVDC}}(s), \tag{3}$$

where $\Delta P_{\text{tie } ij\text{AC}}$ and $\Delta P_{\text{tie } ij\text{HVDC}}$ are the power change through AC and HVDC links.

The proposed PI-TIDN controller is augmented by the HCSA technique subjecting to integral squared error (ISE):

$$\eta_{\text{ISE}} = \int\limits_0^t \left\{(\Delta F_j)^2 + (\Delta P_{j-k})^2\right\} \mathrm{d}t. \tag{4}$$

3. The proposed cascade PI-TIDN controller

A cascade control system is characterized by having two control loops that can be independently tuned, as depicted in Fig. 1b [41]. The primary loop serves as the master, managing the system's final output, while the secondary loop mitigates internal process disturbances. The transfer function equations for the PI-TIDN controller are provided in equations (5) and (6)

$$G_{\text{PI}}(s) = K_{P1i} + \left(\frac{K_{I1i}}{s}\right) + K_{D1i}s, \tag{5}$$

$$G_{\text{TIDN}}(s) = K_{T1i} \left(\frac{1}{s}\right)^{n2i} + \frac{K_{I2i}}{s} + K_{D2i}s\left(\frac{N_{2i}}{s + N_{2i}}\right). \tag{6}$$

The suggested PI-TIDN controller parameters are augmented by the HCSA technique subjected to:

$$0 \leqslant \text{Proportional}(K_{P1i}), \text{Integral}(K_{I1i}, K_{I2i}), \text{Derivative}(K_{D2i}), \text{Tilt}(K_{T2i}) \leqslant 1,$$

$$0 \leqslant \text{Tilt Coefficient}(n_{2i}) \leqslant 7, \quad \text{and} \quad 0 \leqslant \text{Filter}(N_i) \leqslant 100. \tag{7}$$

4. Optimization techniques

4.1. Crow search algorithm

The Crow Search Algorithm (CSA) is an optimization technique inspired by crows' behavior, particularly their food storage skills [38]. In CSA, each crow represents a potential solution, and the algorithm iteratively refines these solutions by mimicking the crows' memory strategies. Each crow remembers its best position, using a probabilistic approach to decide whether to adopt another crow's solution or explore independently. CSA has several advantages, including its straightforward implementation with minimal parameter tuning, making it adaptable to various applications. Its global search capability effectively explores the entire search space, reducing the risk of getting trapped in local optima. Additionally, CSA is versatile for continuous, discrete, and combinatorial problems. The memory feature helps maintain population diversity and prevents premature convergence, leading to faster convergence rates than other optimization methods [38]. The brief about CSA is provided in [38]. It generates a Z-dimension search space set given by

$$
\begin{aligned}
Z^{q,\text{iter}} = \left[Z_1^{q,\text{iter}}, \ Z_2^{q,\text{iter}}, \ \ldots, \ Z_d^{q,\text{iter}} \right] \quad \text{where} \\
q = 1, 2, \ldots, n \quad \text{and} \quad \text{iter} = 1, 2, \ldots, \text{max}_{\text{iter}} \, .
\end{aligned}
\tag{8}
$$

In an iteration, all the agents track and save the food's whopping place's memory (m). Crow has two options when it comes to visiting the whopping place.

Option-1:

Crow-a is unrelated to crow-b, reaching its whopping residence as follows

$$
Z^{a,\text{iter}+1} = Z^{a,\text{iter}} + r_a \times \text{FL}^{a,\text{iter}} \times (m^{b,\text{iter}} - X^{b,\text{iter}}) \quad \text{random}_b \geqslant \text{AP}^{b,\text{iter}}.
\tag{9}
$$

Flight length (FL) determines local-global optima. Intensification and diversification are resolved by awareness probability (AP). Less AP results in intensification and step reductions result in diversification.

Option-2:

Knowing the follow of Crow-b, Crow-a flew to a new position and was assigned as

$$
Z^{a,\text{iter}+1} = \text{random position}.
\tag{10}
$$

The attained ideal values using (9) and (10) are stowed and will be checked for termination criteria. The CSA flow chart is presented in Fig. 2.
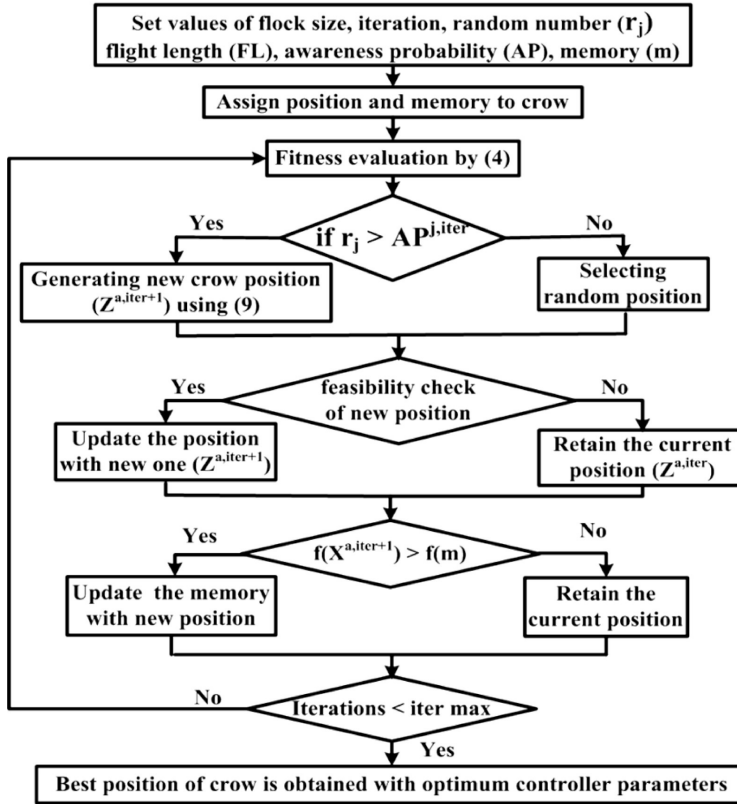
Figure 2: Flowchart of CSA

4.2. Particle swarm optimization

Particle Swarm Optimization (PSO) mimics the bird's social behavior. In PSO, particles are randomly initialized in the solution space. Each particle adjusts its location, which is grounded on its best-known position in the swarm's findings. This involves modifying its velocity to explore the solution space effectively. The algorithm iteratively refines particle positions until it meets a stopping criterion, making PSO well-suited for complex optimization problems. The mathematical expression of PSO in x-dimension can be given by [36]

$$[x_i^t = x_{i,1}^t, \ x_{i,j}^t, \ \ldots, \ x_{i,d}^t], \quad i = 1, 2, \ldots, a. \tag{11}$$

The current resolution of the particle is restructured in terms of local $(P_{i,j})$ – global $(P_{g\,\text{best}})$ bests and is represented by:

$$v_{i,j}^{t+1} = \omega.v_{i,j}^t + C_1.r_1|(p_{i,j}^t - x_{i,j}^t)| + |c_2.r_2(p_{g\,\text{best}\,j}^t - x_{i,j}^t), \tag{12}$$

$$x_{i,j}^{t+1} = x_{i,j}^t + v_{i,j}^{t+1}, \tag{13}$$

where element (j), with inertia (ω) which promotes convergence. The current and best solution during a time (t), velocity (v), random (r), and cognitive (C_1, C_2). The PSO flow chart is shown in Fig. 3.
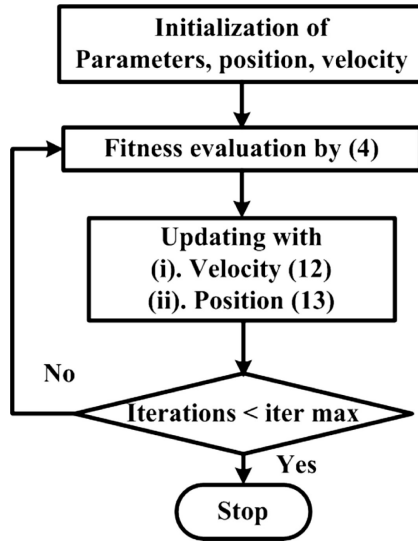

Figure 3: Flowchart of PSO

4.3. Hybrid crow search with particle swarm algorithm

To hybridize the CSA with PSO, follow these steps:

Initialization: Randomly initialize a population of particles (solutions) and define parameters for both algorithms.

Fitness Evaluation: Particle's fitness evaluation using objective function.

PSO Updates: Update particle velocities and positions based on personal best and global best positions using PSO formulas.

Crow Search Updates: Allow crows to explore the solution space, updating their positions based on intelligence and memory.

Hybrid Strategy: Combine updates from both algorithms. For example, alternate between PSO and CSA updates or allow some particles to adopt positions based on the best crow positions.

Selection and Iteration: Evaluate fitness after updates, select the best solutions, and repeat until termination criteria are met.

In this study, the optimum values from CSA are saved and updated with (12) and (13), which promotes convergence speed. If the current fitness is discovered to be superior to a prior solution, current values get updated, and the cycle is repeated until an optimal solution is achieved [42]. The HCSA flow chart is presented in Fig. 4.
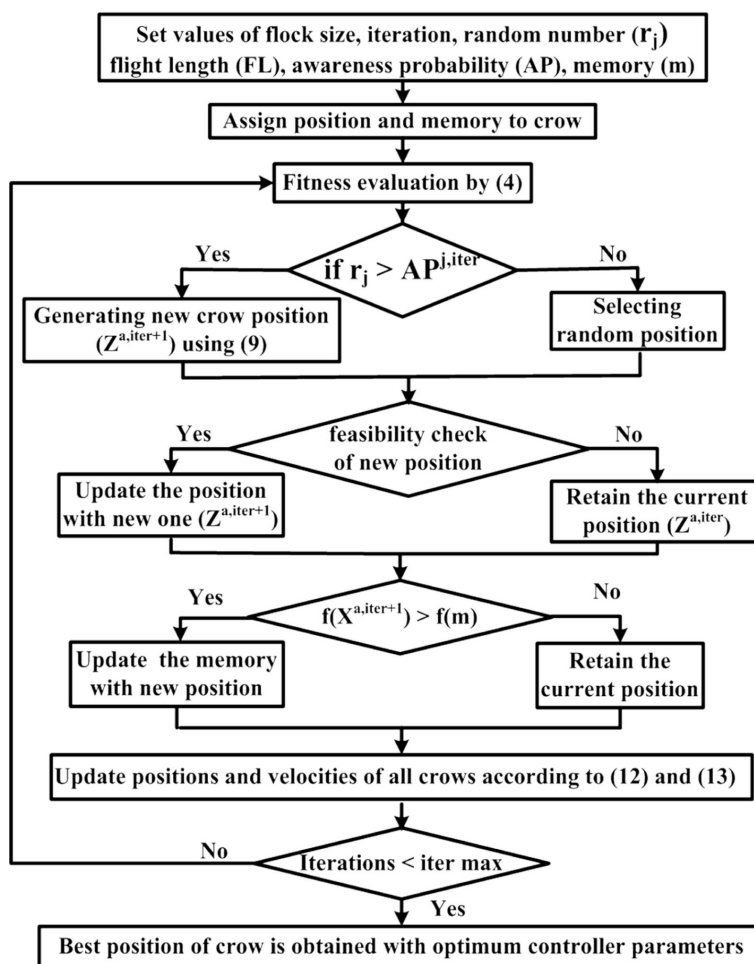
Figure 4: Flowchart of HCSA

5.   Results and Discussions

The MATLAB toolbox is used to perform investigations on the test system. A GDB of 0.0006 p.u and GRC are considered for the thermal system. Investigations are on thermal systems with various controllers. Later, studies were carried out on various wind velocities on WTS units. Investigations are also carried out with HVDC, as well as sensitivity analyses.

5.1.   Thermal system dynamics with PID, TIDN, and proposed PI-TIDN controller

The thermal system is employed with PIDN, TIDN, and the proposed PI-TIDN controller. The HCSA is utilized to optimize controller values. The acquired values are noted in Table 1, and the responses are in Fig. 5. It is perceived that the

reactions with cascade PI-TIDN controller have shown significant improvement in system dynamics.
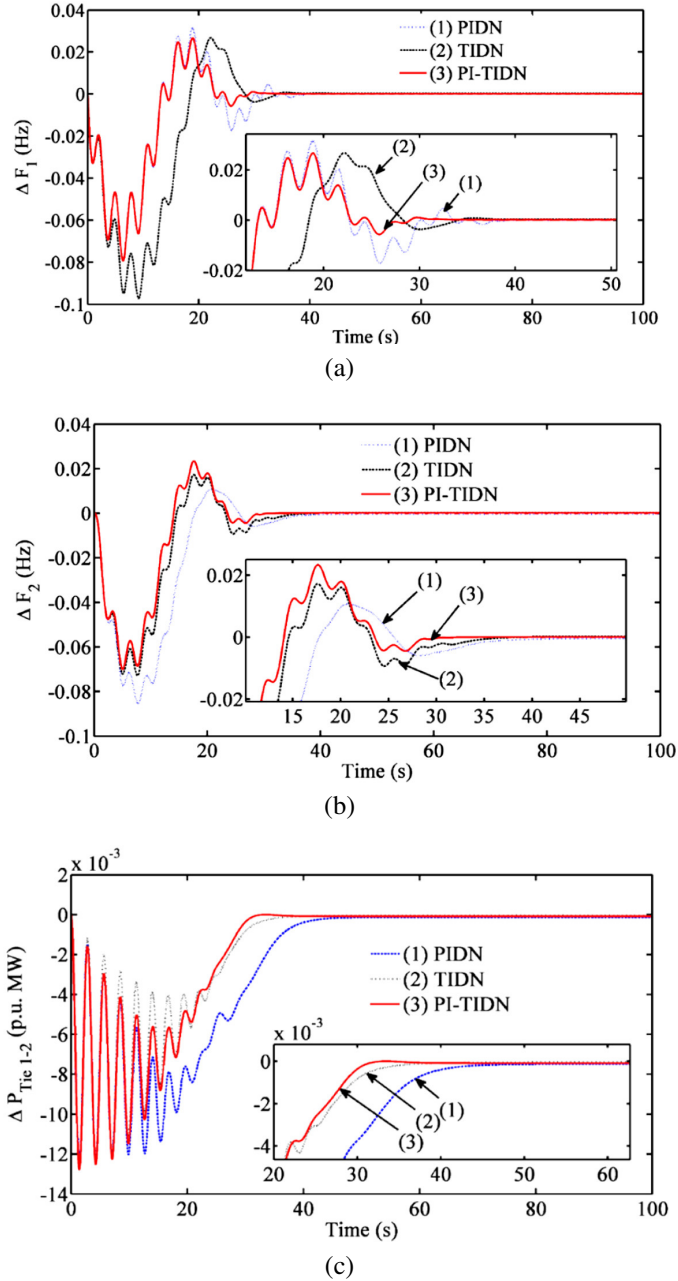

Figure 5: Dynamic responses with PIDN, TIDN, and PI-TIDN controllers (a) ΔF_1, (b) ΔF_2, and (c) $\Delta P_{\text{tie1-2}}$

Table 1: HCSA optimized controller gains of the thermal system

PIDN controller
K_{P1} = 0.3909; K_{I1} = 0.8313; K_{D1} = 0.8033; N_1 = 29.1984; K_{P2} = 0.060; K_{I2} = 0.3992; K_{D2} = 0.5268; N_2 = 43.1651; K_{P3} = 0.4167; K_{I3} = 0.6568; K_{D3} = 0.6279; N_3 = 1.54871
TIDN controller
K_{T1} = 0.3144; n_1 = 4.4208; K_{I1} = 0.0278; K_{D1} = 0.05477; N_1 = 65.421; K_{T2} = 0.7605; n_2 = 4.2293; K_{I2} = 0.5984; K_{D2} = 0.2815; N_2 = 96.450; K_{T3} = 0.7858; n_3 = 3.4636; K_{I3} = 0.7827; K_{D3} = 0.7620, N_3 = 57.1045
PI-TIDN controller
K_{P11} = 0.7293; K_{I11} = 0.4014; K_{T21} = 0.9770; n_{21} = 2.3412; K_{I12} = 0.7467; K_{D12} = 0.2610; N_1 = 85.124; K_{P12} = 0.0108; K_{I12} = 0.9017; K_{T22} = 0.4042; n_{22} = 3.1450; K_{I22} = 0.4493; K_{D22} = 0.9778; N_2 = 12.4578; K_{P13} = 0.1491; K_{I13} = 0.0080; K_{T23} = 0.7300; n_{23} = 1.5460; K_{I23} = 0.0941; K_{D23} = 0.0882, N_3 = 15.1240

5.2. Convergence characteristic assessment among CSA, PSO, and HCSA

In Section 5.1, the thermal system is equipped with a PI-TIDN controller, and its gains are optimized using CSA, PSO, and HCSA individually. Table 2 presents

Table 2: Optimum PI-TIDN controller values with CSA, PSO, and HCSA algorithms

With PSO technique
K_{P11} = 0.1845; K_{I11} = 0.4844; K_{T21} = 0.1398; n_{21} = 6.9821; K_{I12} = 0.0084; K_{D12} = 0.9301; N_1 = 17.8568; K_{P12} = 0.2842; K_{I12} = 6236; K_{T22} = 0.2959; n_{22} = 3.3576; K_{I22} = 0.4934; K_{D22} = 0.1485; N_2 = 61.4292; K_{P13} = 0.8780; K_{I13} = 0.1189; K_{T23} = 0.6959; n_{23} = 6.3283; K_{I23} = 0.4295; K_{D23} = 0.2774; N_3 = 21.5159
With CSA technique
K_{P11} = 0.7182; K_{I11} = 0.0533; K_{T21} = 0.1821; n_{21} = 1.1563; K_{I12} = 0.0191; K_{D12} = 0.4593; N_1 = 65.8639; K_{P12} = 0.1790; K_{I12} = 0.1257; K_{T22} = 0.4546; n_{22} = 0.4856; K_{I22} = 0.7082; K_{D22} = 0.8193; N_2 = 18.8838; K_{P13} = 0.8299; K_{I13} = 0.1050; K_{T23} = 0.4512; n_{23} = 1.1090; K_{I23} = 0.5726; K_{D23} = 0.5996; N_3 = 43.6222
With HCSA technique
K_{P11} = 0.7293; K_{I11} = 0.4014; K_{T21} = 0.9770; n_{21} = 2.3412; K_{I12} = 0.7467; K_{D12} = 0.2610; N_1 = 85.124; K_{P12} = 0.0108; K_{I12} = 0.9017; K_{T22} = 0.4042; n_{22} = 3.1450; K_{I22} = 0.4493; K_{D22} = 0.9778; N_2 = 12.4578; K_{P13} = 0.1491; K_{I13} = 0.0080; K_{T23} = 0.7300; n_{23} = 1.5460; K_{I23} = 0.0941; K_{D23} = 0.0882; N_3 = 15.1240

the optimized values, while Fig. 6 illustrates the corresponding responses. The results in Fig. 6 indicate that HCSA converges more quickly than the other methods.
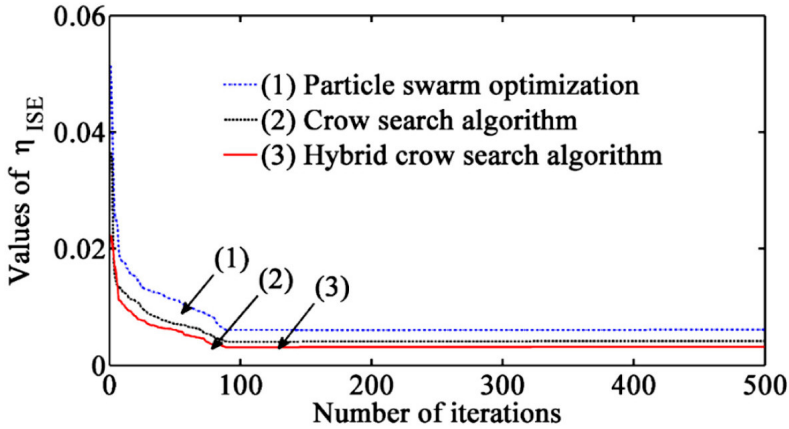

Figure 6: Convergence curves with PSO, CSA, and HCSA algorithm

5.3. Effect of AC-HVDC

An HVDC is linked to the thermal-WTS system to improve the inter-area power transfer capability, forming a parallel AC-HVDC. The best values of PI-TIDN are noted in Table 3. Obtained responses in Fig. 7 show that with parallel AC-HVDC, deviations are reduced over the AC system.
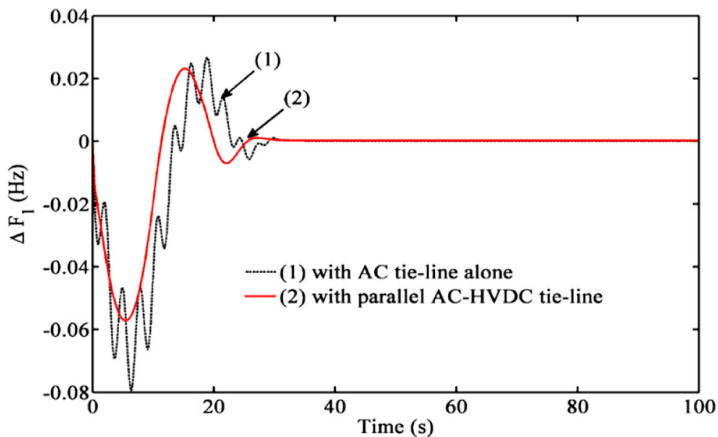
Figure 7: (a)
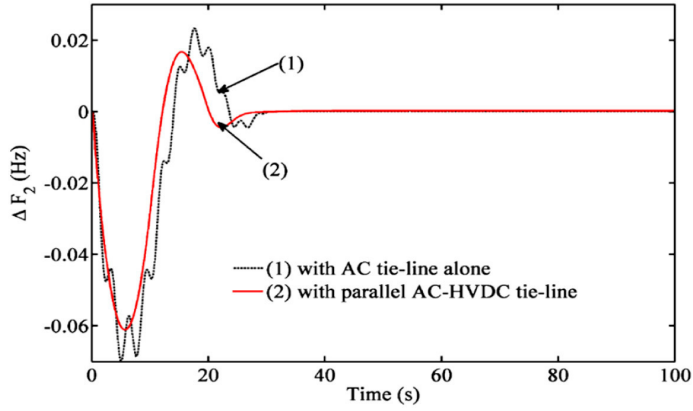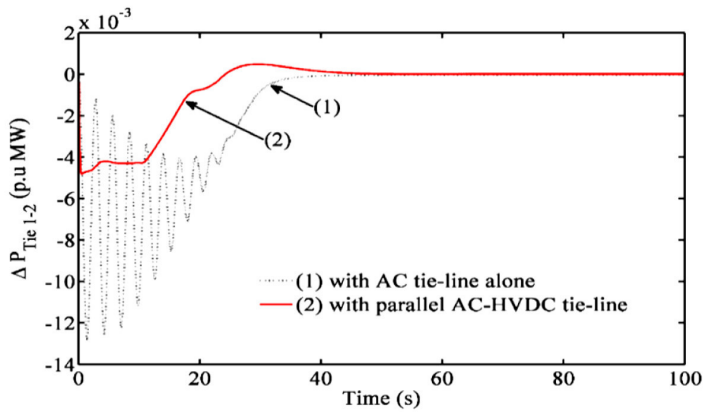
Figure 7: Dynamics with AC-HVDC (a) ΔF_1, (b) ΔF_2 and (c) $\Delta P_{\text{tie1-2}}$

Table 3: HCSA optimized PI-TIDN controller with parallel AC-HVDC system

$K_{P11} = 0.5584$; $K_{I11} = 0.5208$; $K_{T21} = 0.2842$; $n_{21} = 0.643$; $K_{I12} = 0.3392$; $K_{D12} = 0.8807$; $N_1 = 72.842$; $K_{P12} = 0.1066$; $K_{I12} = 0.4376$; $K_{T22} = 0.0163$; $n_{22} = 1.7635$; $K_{I22} = 0.68900$; $K_{D22} = 0.7140$; $N_2 = 89.592$; $K_{P13} = 0.0660$; $K_{I13} = 0.0013$; $K_{T23} = 0.3696$; $n_{23} = 1.8668$; $K_{I23} = 0.6819$; $K_{D23} = 0.5105$; $N_3 = 85.2600$

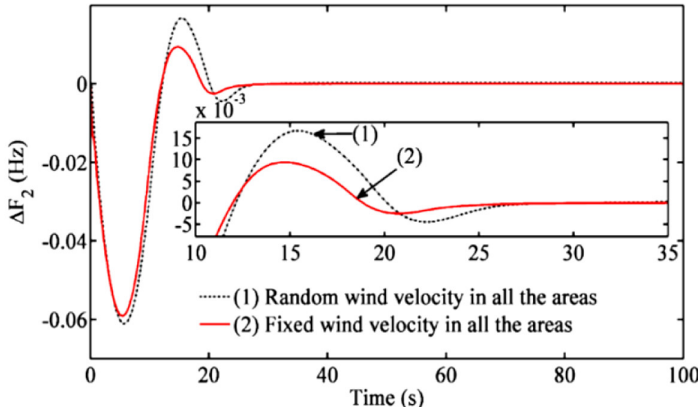### 5.4.   Effect of various wind velocities on WTS units

The thermal system in the above studies is integrated with WTS. Random and fixed wind velocities are given to the WTS unit separately. Table 4 lists the HCSA-optimized PI-TIDN. Dynamic in Fig. 8 suggests that fixed velocities have shown better responses over random velocity.
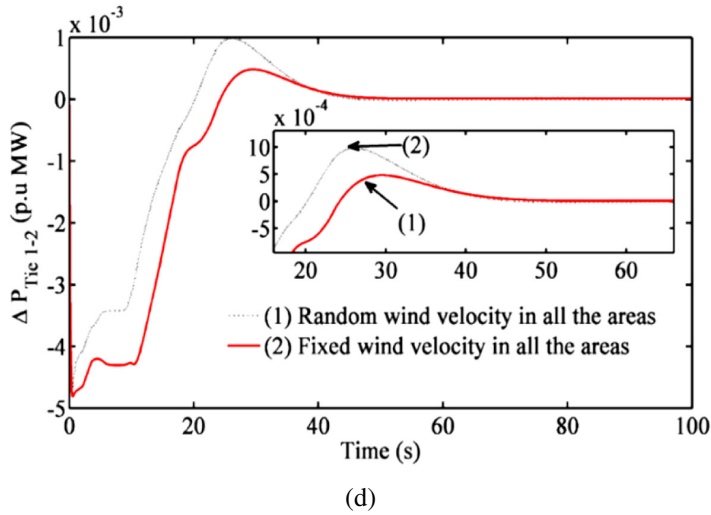
(a)

(b)

(c)

Figure 8: (a)–(c)

(d)
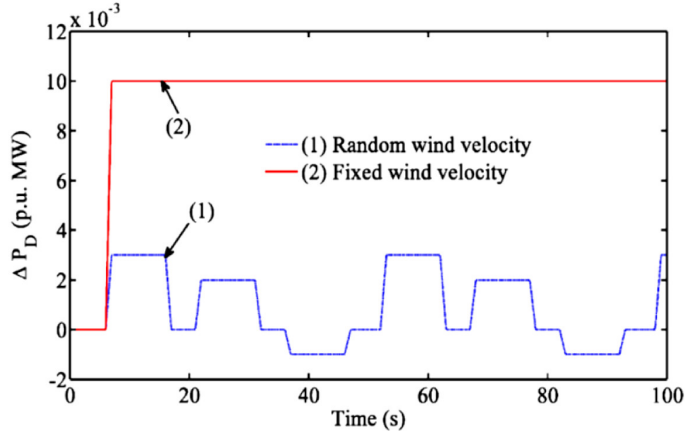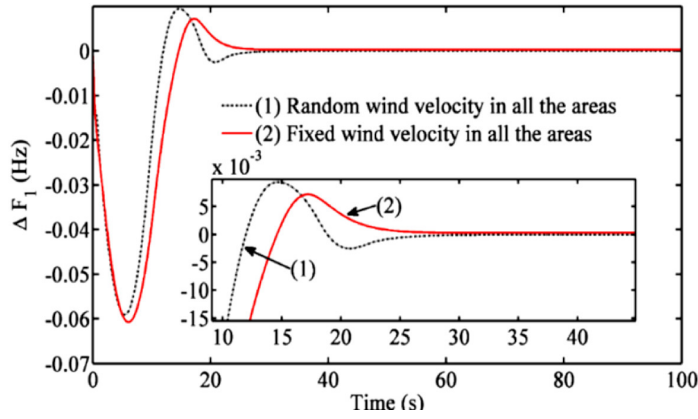
Figure 8: System dynamics with various wind velocities (a) various velocities, (b) ΔF_1, (c) ΔF_2 and (d) $\Delta P_{\text{tie}1-2}$

Table 4: HCSA optimized PI-TIDN controller with various wind velocities in a thermal-WTS

With random wind velocity
$K_{P11} = 0.9085$; $K_{I11} = 0.0518$; $K_{T21} = 0.6654$; $n_{21} = 4.4255$; $K_{I12} = 0.01776$; $K_{D12} = 0.8318$;
$N_1 = 65.3363$; $K_{P12} = 0.1667$; $K_{I12} = 0.3548$; $K_{T22} = 0.152$; $n_{22} = 6.6634$; $K_{I22} = 0.1295$;
$K_{D22} = 0.2321$; $N_2 = 74.1635$; $K_{P13} = 0.8334$; $K_{I13} = 0.2476$; $K_{T23} = 0.0840$; $n_{23} = 602173$;
$K_{I23} = 0.4869$; $K_{D23} = 0.6143$; $N_3 = 30.3816$
With fixed wind velocity
$K_{P11} = 0.6995$; $K_{I11} = 0.8604$; $K_{T21} = 0.5525$; $n_{21} = 6.0214$; $K_{I12} = 0.9239$; $K_{D12} = 0.8753$;
$N_1 = 94.1255$; $K_{P12} = 0.2565$; $K_{I12} = 0.4247$; $K_{T22} = 0.9199$; $n_{22} = 3.6419$; $K_{I22} = 0.2697$;
$K_{D22} = 0.39131$; $N_2 = 177165$; $K_{P13} = 0.1032$; $K_{I13} = 0.0022$; $K_{T23} = 0.4578$; $n_{23} = 6.1561$;
$K_{I23} = 0.3918$; $K_{D23} = 0.9838$; $N_3 = 71.1014$

5.5. System dynamic responses with the integration of WTS unit

Section 5.2 shows the thermal system. WTS is incorporated along with the thermal system in all the areas with fixed wind velocity as input. PI-TIDN controller and HCSA technique are used for optimization. Obtained responses are plotted in Fig. 9 and are compared with the thermal system alone. Investigations reveal that thermal WTS enhances system dynamics.
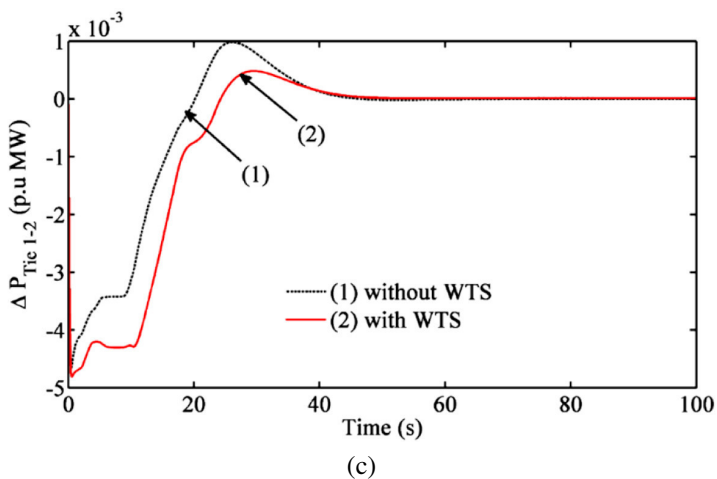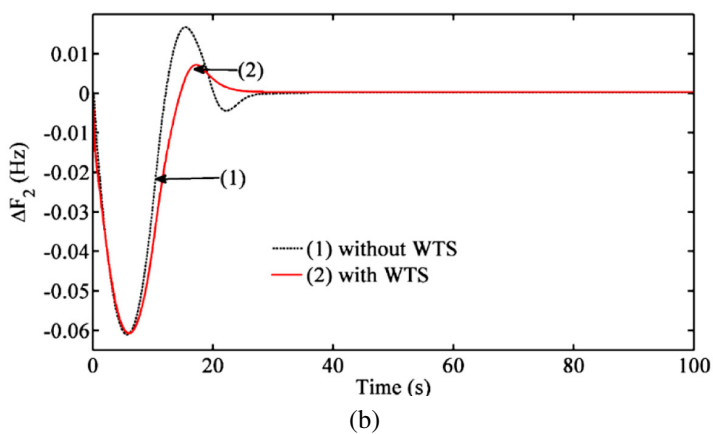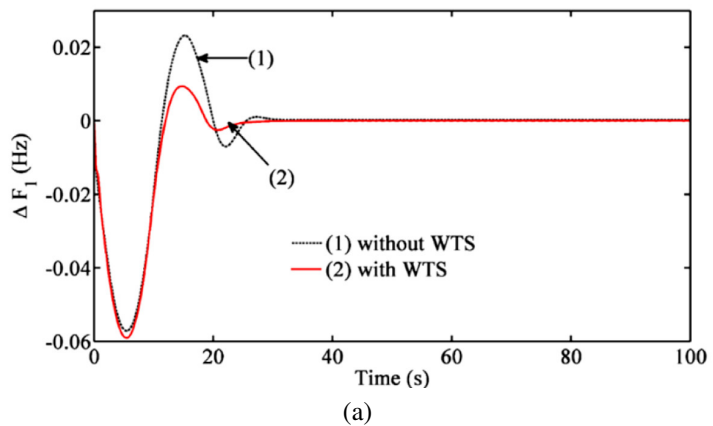
Figure 9: Dynamics considering WTS units (a) ΔF_1, (b) ΔF_2 and (c) $\Delta P_{\text{tie1-2}}$

5.6. Sensitivity analysis of the proposed cascade PI-TIDN controller

Figure 1 is exposed to disparities in inertia and loading conditions from nominal values. Investigations are performed with PI-TIDN and HCSA techniques, and their responses are shown in Fig. 10. The gained responses are related to the system at varied conditions considering optimum values obtained in Section 5.5. Figure 10 suggests that the proposed PI-TIDN controller is vigorous.
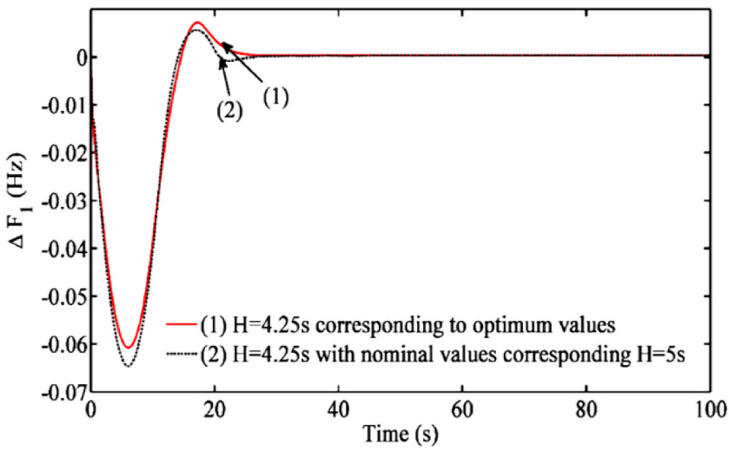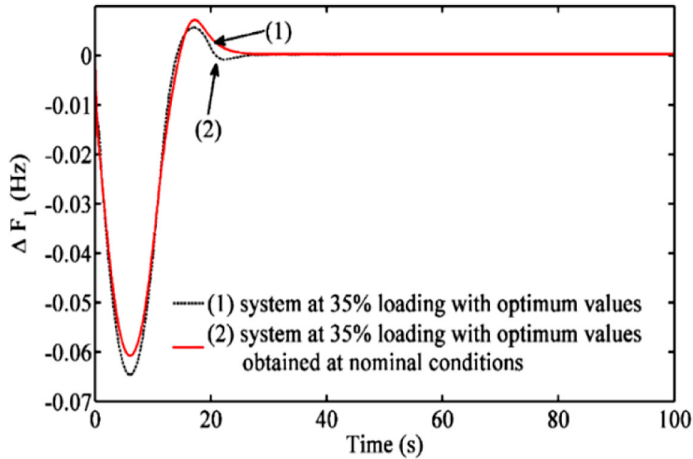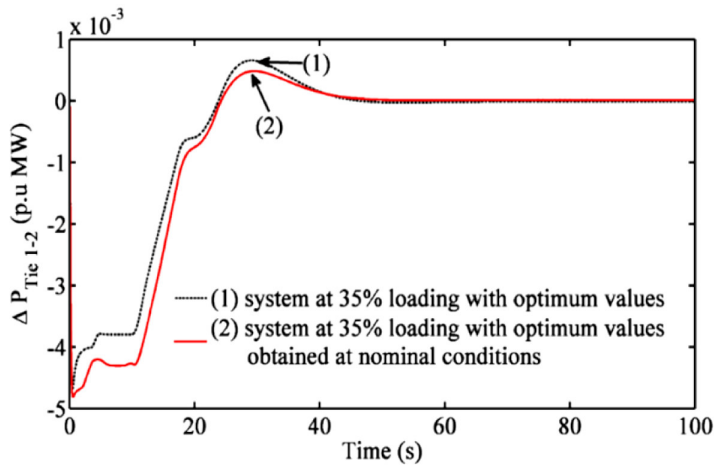

(a)
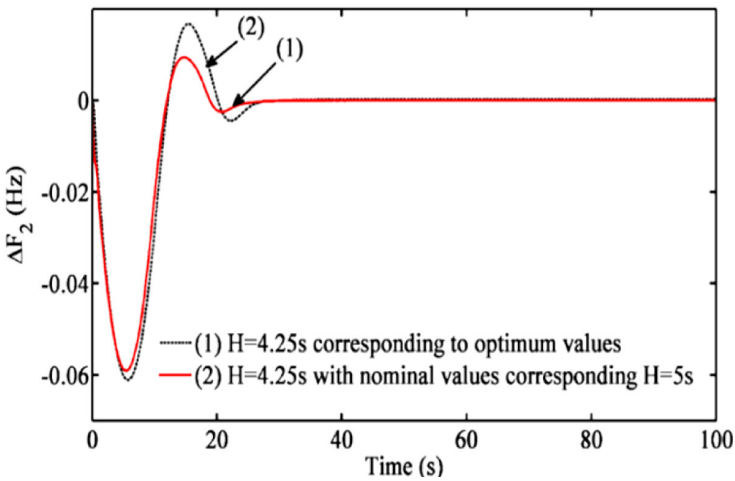
(b)

Figure 10: (a), (b)

(c)

(d)

Figure 10: System dynamics considering sensitivity analysis; inertia variations in (a) ΔF_1 and (b) ΔF_2; loading condition variations in (c) ΔF_1 and (d) $\Delta P_{\text{tie}1\text{-}2}$

6.   Conclusions

An effort was made to design a cascade PI-TIDN controller as a secondary component in AGC studies, utilizing the Hybrid Crow Search Algorithm (HCSA). A comparative analysis shows that the thermal system with the proposed PI-TIDN controller outperforms both the PIDN and TIDN controllers. Additionally, studies conducted with varying wind velocities in wind turbine systems (WTS) indicate that a fixed wind velocity across all areas improves system dynamics

compared to random wind velocities. Furthermore, the integration of WTS and HVDC enhances system performance compared to thermal systems alone and thermal-WTS units. Lastly, sensitivity analysis under different inertia and loading conditions demonstrates that the proposed PI-TIDN controller is vigorous.

Nomenclature

AGC   automatic generation control
CSA   crow search algorithm
HCSA   hybrid crow search algorithm
HVDC   high voltage direct current
PSO   particle swarm optimization
PUS   peak undershoot
RES   renewable energy sources
SA   sensitivity analysis
WTS   wind turbine system
Δ deviations

References

[1] O.I. Elgerd: *Electric Energy Systems Theory: An Introduction*. New Delhi, Tata McGraw-Hill, 2007.

[2] P. Kundur: *Power System Stability and Control*. New Delhi, Tata McGraw Hill, 1993.

[3] O.I. Elgerd and C.E. Fosha: Optimum megawatt-frequency control of multi-area electric energy systems. *IEEE Transactions on Power Apparatus and Systems*, **89**(4), (1970), 556–563. DOI: 10.1109/TPAS.1970.292602

[4] H. Golpira, H. Bevrani and H. Golpira: Application of GA optimization for automatic generation control design in an interconnected power system. *Energy Conversion and Management*, **52**(5), (2011) 2247–2255. DOI: 10.1016/j.enconman.2011.01.010

[5] J. Nanda, A. Mangla and S. Suri: Some new findings on automatic generation control of an interconnected hydrothermal system with conventional controllers. *IEEE Transactions on Energy Conversion*, **21**(1), (2006), 187–194. DOI: 10.1109/TEC.2005.853757

[6] N.R. Babu, T. Chiranjeevi, A. Saha and S.K. Bhagat: Comparative analysis of various energy storage systems in a conventional LFC system considering RDSTS, PWTS and AHVDC models. *Journal of Engineering Research*, **1**(4), (2023), 425–436. DOI: 10.1016/j.jer.2023.100123

[7] M. Javad, Z. Kazem and T.H. Mehrdad: Applying fractional order PID to design TCSC-based damping controller in coordination with automatic generation control of interconnected multi-source power system. *Engineering Science and Technology, an International Journal*, **20**(1), (2017), 1–17. DOI: 10.1016/j.jestch.2016.06.002

[8] N.R. Babu, T. Chiranjeevi, A. Saha, S.K. Bhagat, U.K. Gupta and R.I. Vais: Crow search algorithm optimized cascade controller in a multi-area thermal wind integrated system and its real-time validation. *Electrica*, **23**(3), (2023), 429–437. DOI: 10.5152/electr.2023.22137

[9] N.R. Babu, T. Chiranjeevi, R. Devarapalli, L. Knypiński and P.G. Marquez: Real-time validation of an automatic generation control system considering HPA-ISE with crow search algorithm optimized cascade FOPDN-FOPIDN controller. *Archives of Control Sciences*, **33**(2), 371–390. DOI: 10.24425/acs.2023.146280

[10] E. Rakhshani, K. Rouzbehi, M.A. Elsaharty and P.R. Cortes: Heuristic optimization of supplementary controller for VSC-HVDC/AC interconnected grids considering PLL. *Electric Power Components and Systems*, **45**(3), (2017), 288–301. DOI: 10.1080/15325008.2016.1232765

[11] J. Zhu, J.M. Guerrero, W. Hung, C.D. Booth and G.P. Adam: Generic inertia emulation controller for multi-terminal voltage-source-converter high voltage direct current systems. *IET Renewable Power Generation*, **8**(7), (2014), 740–748. DOI: 10.1049/iet-rpg.2014.0109

[12] A. Prakash, S. Murali, R. Shankar and R. Bhushan: HVDC tie-link modeling for restructured AGC using a novel fractional order cascade controller. *Electric Power Systems Research*, **170** (2019), 244–258. DOI: 10.1016/j.epsr.2019.01.021

[13] N.R. Babu, T. Chiranjeevi, R. Devarapalli and S.K. Bhagat: Optimal location of FACTs devices in LFC studies considering the application of RT-Lab studies and Emperor Penguin optimization algorithm. *Journal of Engineering Research*, **11**(2), (2023). DOI: 10.1016/j.jer.2023.100060

[14] O.D. Adeuyi, M. Cheah-Mane, J. Liang, N. Jenkins, Y. Wu, C. Li and X. Wu: Frequency support from modular multilevel converter based multi-terminal HVDC schemes. *IEEE Power and Energy Society General Meeting*, Denver, (2015), 1–5. DOI: 10.1109/PESGM.2015.7286086

[15] N. Pathak, A. Verma, T.S. Bhatti and I. Nasiruddin: Modeling of HVDC tie links and their utilization in AGC/LFC operations of multi-area power systems. *IEEE Transactions on Industrial Electronics*, **66**(3), (2019), 2185–2197. DOI: 10.1109/TIE.2018.2835387

[16] N.R. Babu, S.K. Bhagat, L.C. Saikia and T. Chiranjeevi: Application of hybrid crow-search with particle swarm optimization algorithm in AGC studies of multi-area systems. *Journal of Discrete Mathematical Sciences and Cryptography*, **23**(2), (2020), 429–439. DOI: 10.1080/09720529. 2020.1728896

[17] L.C. Saikia, A. Chowdhury, N. Shakya, S. Shukla and P.K. Soni: AGC of a multi area gas-thermal system using firefly optimized IDF controller. *Annual IEEE India Conference*, Mumbai, India, (2013), 1–6. DOI: 10.1109/INDCON.2013.6725998

[18] G. Sharma, Ibraheem, K.R. Niazi and R.C. Bansal: Adaptive fuzzy critic based control design for AGC of power system connected via AC/DC tie-lines. *IET Generation, Transmission and Distribution*, **11**(2), (2016), 560–569. DOI: 10.1049/iet-gtd.2016.1164

[19] G. Sharma, I. Nasiruddin and K.R. Niazi: Robust automatic generation control regulators for a two-area power system interconnected via AC/DC tie-lines considering new structures of matrix Q. *IET Generation, Transmission and Distribution*, 10(14), (2016), 3570–3579. DOI: 10.1049/iet-gtd.2016.0321

[20] K. Jagatheesan, B. Anand, Sourav Samanta, N. Dey, A.S. Ashour and V.E. Balas: Design of a proportional-integral-derivative controller for an automatic generation control of multi-area power thermal systems using firefly algorithm. *IEEE/CAA Journal of Automatica Sinica*, **6**(2), (2019), 503–515. DOI: 10.1109/JAS.2017.7510436

[21] I. Pan and S. Das: Fractional order AGC for distributed energy resources using robust optimization. *IEEE Transactions on Smart Grid*, **7**(5), (2016), 2175–2186. DOI: 10.1109/TSG.2015.2459766

[22] P.N. Topno and S. Chanana: Tilt integral derivative control for two-area load frequency control problem. *2nd International Conference on Recent Advances in Engineering and Computational Sciences*, Chandigarh, India, (2015), 1–6.

[23] S.K. Bhagat, S. Behera, A. Saha, T. Bal, T. Chiranjeevi, R. Devarapalli and N.R. Babu: Bird swarm algorithm optimized TIDD controller for multi-area load frequency control application. *SN Computer Science*, **4** (2023), 138. DOI: 10.1007/s42979-022-01556-5

[24] N.R. Babu, S.K. Bhagat, T. Chiranjeevi, M. Pushkarna, A. Saha, H. Kotb, K.M. Abo-Ras, F. Alsaif, S. Alsulamy, Y.Y. Ghadi and D.T. Hermann: Frequency control of a realistic Dish Stirling Solar Thermal System and accurate HVDC models using a cascaded FOPI-IDDN based crow-search algorithm. *International Journal of Energy Research*, (2023), 1–18. DOI: 10.1155/2023/9976375

[25] A. Saha, P. Dash, N.R. Babu, T. Chiranjeevi, B. Venkateswararao and Ł. Knypiński: Impact of spotted hyena optimized cascade controller in load frequency control of wave-solar-double compensated capacitive energy storage based interconnected power system. *Energies*, **15**(19), (2022). DOI: 10.3390/en15196959

[26] A. Saha, P. Dash, N.R. Babu, T. Chiranjeevi, M. Dhananjaya and Ł. Knypiński: Dynamic stability evaluation of an integrated biodiesel-geothermal power plant-based power system with spotted hyena optimized cascade controller. *Sustainability*, **14**(22), (2022). DOI: 10.3390/su142214842

[27] A. Nocoń, S. Paszek and P. Pruski: Multi-criteria optimization of the parameters of PSS3B system stabilizers operating in an extended power system with the use of a genetic algorithm. *Archives of Control Sciences*, **32**(2), (2022), 233–255. DOI: 10.24425/acs.2022.141711

[28] T. Chiranjeevi and U.K. Gupta: Ideal parameter distribution in renewable integrated rapid charging electric vehicle station. *Energy Sources, Part A: Recovery, Utilization, and Environmental Effects*, **45**(1), (2023), 888–904. DOI: 10.1080/15567036.2023.2174614

[29] M. Ahsan, D. Bismor and M.A. Manzoor: ARL-wavelet-BPF optimization using PSO algorithm for bearing fault diagnosis. *Archives of Control Sciences*, **33**(3), (2023), 589–606. DOI: 10.24425/acs.2023.146961

[30] R.I. Vais, K. Sahay, T. Chiranjeevi, R. Devarapalli and Ł. Knypiński: Parameter extraction of solar photovoltaic modules using a novel bio-inspired swarm intelligence optimisation algorithm, *Sustainability*, **15**, 8407. DOI: 10.3390/su15108407

[31] A. Sahan and L.C. Saikia: Utilization of ultra-capacitor in load frequency control under restructured STPP-thermal power systems using WOA optimized PIDN-FOPD controller. *IET Generation, Transmission and Distribution*, **11**(13), (2017), 3318–3331. DOI: 10.1049/iet-gtd.2017.0083

[32] W. Tasnin and L.C. Saikia: Maiden application of an sine–cosine algorithm optimised FO cascade controller in automatic generation control of multi-area thermal system incorporating dish-Stirling solar and geothermal power plants. *IET Renewable Power Generation*, **12**(5), (2018), 585–597. DOI: 10.1049/iet-rpg.2017.0063

[33] M. Raju, L.C. Saikia, N. Sinha and D. Saha: Application of ant-lion optimizer technique in restructured automatic generation control of two-area hydro-thermal system considering governor dead band. *Conference on Innovations in Power and Advanced Computing Technologies*, Vellore, India, (2017). DOI: 10.1109/IPACT.2017.8245099

[34] A. Rahman, L.C. Saikia and N. Sinha: Load frequency control of a hydro-thermal system under deregulated environment using biogeography-based optimized three-degree-of-freedom integral derivative controller. *IET Generation, Transmission and Distribution*, **9**(15), (2015), 2284–2293. DOI: 10.1049/iet-gtd.2015.0317

[35] J. Pierezan and L.D.S. Coelho: Coyote optimization algorithm: A new metaheuristic for global optimization problems. *IEEE Congress on Evolutionary Computation*, Rio de Janeiro, (2018). DOI: 10.1109/CEC.2018. 8477769

[36] J. Kennedy and R. Eberhart: Particle swarm optimization. *Proceedings of ICNN'95 – International Conference on Neural Networks*, Perth, Australia, **4** (1995), 1942–1948. DOI: 10.1109/ICNN.1995.488968

[37] P. Dash, L.C. Saikia and N. Sinha: Comparison of performances of several FACTS devices using Cuckoo search algorithm optimized 2DOF controllers in multi-area AGC. *International Journal of Electrical Power and Energy Systems*, **65** (2015), 316–324. DOI: 10.1016/j.ijepes.2014.10.015

[38] A. Askarzadeh: A novel metaheuristic method for solving constrained engineering optimization problems: Crow search algorithm. *Journal of Computers and Structures*, **169** (2016), 1–12. DOI: 10.1016/j.compstruc. 2016.03.001

[39] S.K. Bhagat, N.R. Babu, L.C. Saikia, T. Chiranjeevi, R. Devarapalli and P.G. Marquez: A review on various secondary controllers and optimization techniques in automatic generation control. *Archives of Computational Methods in Engineering*, **30** (2023), 3081–3111. DOI: 10.1007/s11831-023-09895-z

[40] Ramjug-Ballgobin and C. Ramlukon: A hybrid metaheuristic optimization technique for load frequency control. *SN Applied Sciences*, **3** (2021). DOI: 10.1007/s42452-021-04482-y

[41] N.R. Babu, S.K. Bhagat, L.C. Saikia, T. Chiranjeevi, R. Devarapalli and F.P.G. Márquez: A comprehensive review of recent strategies on automatic generation control/load frequency control in power systems. *Archives of Computational Methods in Engineering*, **30** (2023), 543–572. DOI: 10.1007/s11831-022-09810-y

[42] K.W. Huang and Z.X. Wu: CPO a crow particle optimization algorithm. *International Journal of Computational Intelligence Systems*, **12**(1), (2018), 426–435. DOI: 10.2991/ij-cis.2018.125905658